Distributed IRS With Statistical Passive Beamforming for MISO Communications

Yuwei Gao, Jindan Xu, *Member, IEEE*, Wei Xu, *Senior Member, IEEE*, Derrick Wing Kwan Ng, *Senior Member, IEEE*, and Mohamed-Slim Alouini, *Fellow, IEEE*

***Abstract*—Intelligent reflecting surface (IRS) has recently been identified as a prominent technology with the ability of enhancing wireless communication by dynamically manipulating the propagation environment. This letter investigates a multiple-input single-output (MISO) system deploying distributed IRSs. For practical considerations, we propose an efficient design of passive reflecting beamforming for the IRSs to exploit statistical channel state information (CSI) and analyze the achievable rate of the network taking into account the impact of CSI estimation error. The ergodic achievable rate is derived in a closed form, which provides insightful system design guidelines. Numerical results confirm the accuracy of the derived results and unveil the performance superiority of the proposed distributed IRS deployment over the conventional centralized deployment.**

***Index Terms*—Intelligent reflecting surface (IRS), ergodic achievable rate, passive beamfoming, channel estimation.**

I. Introduction

As a key technology of the fifth-generation (5G) wireless networks, the merits of massive MIMO are reaped at the cost of increased power consumption and hardware cost [1]. To circumvent these challenges, intelligent reflecting surface (IRS), which is enabled by recent developments in the metamaterial technology, has become a promising alternative to enhance the performance of wireless communication systems by exploiting a passive antenna array [2].

IRS is a reprogrammable metasurface comprising of a large number of cost-effective passive reflecting elements that can dynamically manipulate impinging electromagnetic waves, thereby constructing favorable wireless channels. The IRS can be easily attached to or removed from existing objects in the environment (e.g., walls and ceilings) to serve distant groups of users. As a result, recent studies have focused on the fundamental challenges in applying IRSs in practice, e.g., channel estimation, passive beamforming design, and performance evaluation. For instance, in [3], the authors established a "signal hotspot" as well as an "interference-free zone" by jointly optimizing the reflecting beamformers and the deployment of multiple IRSs. Also, in [4], it was proved that the introduction of an IRS can considerably enhance the spectral efficiency of a large-scale antenna system even with a coarsely discretized reflecting beamformer equipped at the IRS. To fully unlock the potential of IRS, the design of pragmatic channel estimation methods were also investigated for IRS systems [5], [6]. In [7], [8], the ergodic achievable rate was characterized averaged over both channel fading and random IRS/UE locations to investigate the system level performance aided by distributed IRSs. However, most of these studies focused on a centralized deployment of a single IRS, while practical limitations, such as CSI imperfection, have rarely been considered for the design of distributed IRS beamforming. More importantly, a thorough study on the performance of distributed IRS systems has not been reported in the literature yet.

In this letter, we consider a multiple-input single-output (MISO) system assisted by multiple distributed IRSs which exploit statistical CSI, for the design of passive beamforming and the corresponding performance at the receiver is analyzed. In particular, we first propose a low-complexity passive beamforming design for the IRSs which exploit only statistical correlation information of the channels. Then, we analyze the ergodic rate of the network with the considerations of CSI estimation error at the receiver. An exact closed-form expression is obtained for characterizing the ergodic rate. Furthermore, we find that the ergodic rate is significantly improved with the increasing number of line-of-sight (LoS) paths between base station (BS)-to-IRS and IRS-to-user links. The superiority of the distributed IRSs over a centralized IRS is verified since the former increases the possibility of the presence of LoS channels.

Notations: $\mathbb{E}\{\cdot\}$ is the statistical expectation operation. $[\mathbf{H}]_{i,j}$ is the (i, j)th-element of matrix $\mathbf{H}$. Operators $\mathrm{tr}(\cdot)$, $\mathrm{diag}\{\cdot\}$, $\mathrm{blkdiag}\{\cdot\}$, and $\angle$ represent the trace, diagonalization, the block diagonalization of an input matrix, and angle respectively. Operator $\|\cdot\|$ is the Euclidean norm of an input vector. Operator $\otimes$ is the Kronecker product.

Manuscript received August 28, 2020; accepted September 12, 2020. Date of publication September 18, 2020; date of current version February 9, 2021. This work was supported in part by the NSFC under Grant 62022026, Grant 61871109, and Grant 61941115, and in part by the Natural Science Foundation of Jiangsu Province for Distinguished Young Scholars under Grant BK20190012. The work of Derrick Wing Kwan Ng was supported in part by the UNSW Digital Grid Futures Institute, UNSW, Sydney, Under a Cross-Disciplinary Fund Scheme and in part by the Australian Research Council's Discovery Project under Grant DP190101363. The associate editor coordinating the review of this article and approving it for publication was G. Zheng. *(Corresponding author: Wei Xu.)*

Yuwei Gao and Jindan Xu are with the National Mobile Communications Research Laboratory, Southeast University, Nanjing 210096, China (e-mail: 220190879@seu.edu.cn; jdxu@seu.edu.cn).

Wei Xu is with the National Mobile Communications Research Laboratory, Southeast University, Nanjing 210096, China, and also with Purple Mountain Laboratories, Nanjing 211111, China (e-mail: wxu@seu.edu.cn).

Derrick Wing Kwan Ng is with the School of Electrical Engineering and Telecommunications, University of New South Wales, Sydney, NSW 2052, Australia (e-mail: w.k.ng@unsw.edu.au).

Mohamed-Slim Alouini is with the Division of Computer, Electrical, and Mathematical Science and Engineering, King Abdullah University of Science and Technology, Thuwal 23955, Saudi Arabia (e-mail: slim.alouini@kaust.edu.sa).

Digital Object Identifier 10.1109/LWC.2020.3024952

II. System Model

We focus on the case where a typical UE at any arbitrary location in the cell is served by multiple distributed IRSs on the user, compared with a larger-sized centralized IRS with the same total number of antennas on IRSs. We consider a single-user MISO downlink system which consists of one BS and *N* IRSs in a single cell. The BS is equipped with *M* antennas and each IRS has *L* passive reflectors. Assume that the channel between the BS and IRS *n*, $\forall n \in \{1,\ldots,N\}$, follows a correlated Rician distribution, given as

$$\mathbf{H}_n = \sqrt{\frac{\beta_n K_{1,n}}{K_{1,n}+1}}\bar{\mathbf{H}}_n + \sqrt{\frac{\beta_n}{K_{1,n}+1}}\widetilde{\mathbf{H}}_n, \tag{1}$$

where β_n is the large-scale path-loss, $\bar{\mathbf{H}}_n \in \mathbb{C}^{L\times M}$ is the LoS component, $\widetilde{\mathbf{H}}_n \sim \mathcal{CN}(\mathbf{0}, \mathbf{R}_n \otimes \mathbf{I}_M)$ denotes the non-LoS (NLoS) component with spatial correlation, $\mathbf{R}_n \succeq \mathbf{0}$, and $K_{1,n}$ is the Rician *K*-factor. The entry $[\bar{\mathbf{H}}_n]_{i,j} = e^{-j2\pi\frac{d_{n,ij}}{\lambda}}$, where λ is the wave length and $d_{n,ij}$ is the distance between reflecting element *i* of IRS *n* and antenna *j* of the BS. Similarly, we denote the channel between IRS *n* and the user by

$$\mathbf{g}_n = \sqrt{\frac{\alpha_n K_{2,n}}{K_{2,n}+1}}\bar{\mathbf{g}}_n + \sqrt{\frac{\alpha_n}{K_{2,n}+1}}\widetilde{\mathbf{g}}_n, \tag{2}$$

where α_n, $K_{2,n}$, $\bar{\mathbf{g}}_n \in \mathbb{C}^{L\times 1}$, and $\widetilde{\mathbf{g}}_n \sim \mathcal{CN}(\mathbf{0}, \mathbf{I}_L)$ are similarly defined as in (1).

The direct link between the BS and the user, denoted by $\mathbf{h}_d \in \mathbb{C}^{M\times 1}$, is assumed Rayleigh distributed with zero mean and unit variance. For the case where a direct link between the BS and the user is available, the user may better communicate directly with the BS. Then, the received signal at the user is given by[1]

$$y = \sqrt{P}\left(\mathbf{h}_d^H + \sum_{n=1}^{N}\mathbf{g}_n^H\mathbf{\Phi}_n\mathbf{H}_n\right)\mathbf{f}s + w, \tag{3}$$

where $\mathbf{\Phi}_n = \mathrm{diag}\{e^{j\phi_{n,1}},\ldots,e^{j\phi_{n,L}}\}$, $\phi_{n,l} \in [0, 2\pi)$, $\forall l \in \{1,\ldots,L\}$, is the *l*th phase shift introduced by the reflecting beamforms of IRS *n*, P is the transmit power of the BS, w denotes the additive white Gaussian nosie (AWGN) with zero mean and variance σ_w^2, $\mathbf{f} \in \mathbb{C}^{M\times 1}$ is the beamforming vector adopted at the BS, and $s \in \mathbb{C}$ is the source symbol satisfying $\mathbb{E}\{|s|^2\} = 1$. For notational simplicity, we define the stacked channel matrices as $\mathbf{H} = [\mathbf{H}_1^H,\ldots,\mathbf{H}_N^H]^H \triangleq \bar{\mathbf{H}} + \mathbf{K}_1\widetilde{\mathbf{H}}$, where $\bar{\mathbf{H}} = [\sqrt{\frac{\beta_1 K_{1,1}}{K_{1,1}+1}}\bar{\mathbf{H}}_1^H,\ldots,\sqrt{\frac{\beta_N K_{1,N}}{K_{1,N}+1}}\bar{\mathbf{H}}_N^H]^H$ and $\widetilde{\mathbf{H}} = [\widetilde{\mathbf{H}}_1^H,\ldots,\widetilde{\mathbf{H}}_N^H]^H$. It is readily known that $\widetilde{\mathbf{H}} \sim \mathcal{CN}(\mathbf{0}, \mathbf{R}\otimes\mathbf{I}_M)$ with $\mathbf{R} = \mathrm{blkdiag}\{\mathbf{R}_1,\ldots,\mathbf{R}_N\}$ and $\mathbf{K}_1 = \mathrm{blkdiag}\{\sqrt{\frac{\beta_1}{K_{1,1}+1}}\mathbf{I}_L,\ldots,\sqrt{\frac{\beta_N}{K_{1,N}+1}}\mathbf{I}_L\}$. We also define $\mathbf{G} \triangleq \bar{\mathbf{G}} + \mathbf{K}_2\widetilde{\mathbf{G}}$, where $\mathbf{K}_2 = \mathrm{blkdiag}\{\sqrt{\frac{\alpha_1}{K_{2,1}+1}}\mathbf{I}_L,\ldots,\sqrt{\frac{\alpha_N}{K_{2,N}+1}}\mathbf{I}_L\}$, $\bar{\mathbf{G}} = \mathrm{blkdiag}\{\sqrt{\frac{\alpha_1 K_{2,1}}{K_{2,1}+1}}\bar{\mathbf{g}}_1^H,\ldots,\sqrt{\frac{\alpha_N K_{2,N}}{K_{2,N}+1}}\bar{\mathbf{g}}_N^H\}$, and $\widetilde{\mathbf{G}} = \mathrm{blkdiag}\{\widetilde{\mathbf{g}}_1^H,\ldots,\widetilde{\mathbf{g}}_N^H\}$.

[1]We assume that the signals experienced more than one reflections are ignored as they are severely attenuated compared with the directly reflected one [7].

Then, let $\mathbf{v}_n \triangleq [e^{j\phi_{n1}},\ldots,e^{j\phi_{nL}}]^H$, $\forall n \in \{1,\ldots,N\}$, and $\mathbf{G} \triangleq \mathrm{blkdiag}\{\mathbf{g}_1^H,\ldots,\mathbf{g}_N^H\}$. The received signal at the user in (3) can be equivalently rewritten as

$$y = \sqrt{P}\Big(\mathbf{h}_d^H + \mathbf{v}^H\mathbf{Z}\Big)\mathbf{f}s + w, \tag{4}$$

where $\mathbf{v}^H = [\mathbf{v}_1^H,\ldots,\mathbf{v}_N^H]$ and $\mathbf{Z} \triangleq \mathbf{GH}$.

Now, we are ready to present the design of the reflecting beamformer, $\mathbf{v}$, and charaterize its ergodic achievable rate.

III. Distributed IRSs With Statistical CSI

A. Distributed Reflection Design With Statistical CSI

To facilitate the control of the distributed IRSs in practice, we consider that only statistical CSI is available for the design of the reflecting beamformers, $\mathbf{v}$, of the IRSs [10] for maximizing the ergodic achievable rate of the network. From (4), the equivalent SNR of the received signal depends on the availability of CSI, which makes the problem challenging. In general, with limited system resources, the transmitter can acquire only imperfect CSI through a dedicated channel estimation. Consider the application of a typical linear minimum mean-squared error (LMMSE) channel estimate. It follows from the property of MMSE estimation, e.g., [9], [10], that the CSI estimates of the channels, $\mathbf{Z}$ and $\mathbf{h}_d$, can be written as $\mathbf{Z} = \hat{\mathbf{Z}} + \mathbf{E}_{\mathrm{Z}}$ and $\mathbf{h}_d = \hat{\mathbf{h}}_d + \mathbf{e}_d$, respectively, where $\mathbf{E}_{\mathrm{Z}} \sim \mathcal{CN}(\mathbf{0}, \xi\mathbf{I}_{NL}\otimes\mathbf{I}_M)$ and $\mathbf{e}_d \sim \mathcal{CN}(\mathbf{0}, \xi\mathbf{I}_M)$ are, respectively, the corresponding estimation errors. Letting T be the length of training sequences and ρ as the signal-to-noise ratio (SNR) of the training sequence, we have $\xi = \frac{1}{1+T\rho}$ [11]. By exploiting the typical beamforming technique of maximum ratio transmission (MRT) at the BS due to its optimality maximizing the receive SNR in a single-user system, i.e., $\mathbf{f} = \frac{(\hat{\mathbf{h}}_d^H + \mathbf{v}^H\hat{\mathbf{Z}})^H}{\|\hat{\mathbf{h}}_d^H + \mathbf{v}^H\hat{\mathbf{Z}}\|}$, the received signal in (4) becomes

$$y = \left(\|\hat{\mathbf{h}}_d^H + \mathbf{v}^H\hat{\mathbf{Z}}\| + \frac{(\mathbf{e}_d^H + \mathbf{v}^H\mathbf{E}_{\mathrm{Z}})(\hat{\mathbf{h}}_d + \hat{\mathbf{Z}}^H\mathbf{v})}{\|\hat{\mathbf{h}}_d^H + \mathbf{v}^H\hat{\mathbf{Z}}\|}\right)\sqrt{P}s + w. \tag{5}$$

Then, the system ergodic achievable rate can be expressed as

$$C = \mathbb{E}\left\{\log_2\left(1 + P\frac{\|\hat{\mathbf{h}}_d^H + \mathbf{v}^H\hat{\mathbf{Z}}\|^2}{\sigma_w^2 + \frac{|(\mathbf{e}_d^H + \mathbf{v}^H\mathbf{E}_{\mathrm{Z}})(\hat{\mathbf{h}}_d + \hat{\mathbf{Z}}^H\mathbf{v})|^2}{\|\hat{\mathbf{h}}_d^H + \mathbf{v}^H\hat{\mathbf{Z}}\|^2}}\right)\middle|\hat{\mathbf{h}}_d, \hat{\mathbf{Z}}\right\}. \tag{6}$$

The ergodic rate in (6) contains nested integrals over both the channel fading and the CSI estimation errors, which is mathematically intractable. To proceed, we resort to first presenting a tight approximation of (6).

Theorem 1: Given an arbitrary reflecting beamforming design $\mathbf{v}$, the ergodic achievable rate of the network is tightly approximated as

$$\bar{C} = \log_2\left(1 + P\frac{\left|\mathbf{v}^H\mathbf{J}\mathbf{v}\right|^2}{\mathbf{v}^H\mathbf{Q}\mathbf{v}}\right), \tag{7}$$

where $\mathbf{J} \triangleq \frac{\gamma_1}{NL} + \xi MNL + \mathbf{C}$, $\mathbf{Q} \triangleq \frac{\sigma_w^2\gamma_1+\gamma_2}{NL} + (\sigma_w^2 M + \gamma_3)NL\xi + (\sigma_w^2+\gamma_4)\mathbf{C}$, $\mathbf{C}$ is a constant matrix given in (22)

with respect to the channel statistical and the LoS components, and $\gamma_1 \triangleq (1+\xi)M$, $\gamma_2 \triangleq \xi M + \xi^2 M(M+1)$, $\gamma_3 \triangleq \gamma_1 + \xi M + \xi(M+1)MNL$, and $\gamma_4 \triangleq \xi(1+NL)$ are constant system parameters.

Proof: See Appendix A. ∎

For the distributed IRSs and considering limited bandwidth of controlling signals for the IRSs, we design the reflecting beamformers by utilizing statistical CSI. By applying *Theorem 1* and temporarily ignoring the constant-magnitude constrants of $\mathbf{v}$, the problem of optimizing $\mathbf{v}$ can be formulated as:

$$\underset{\mathbf{v}}{\text{maximize}} \quad \frac{\left|\mathbf{v}^H \mathbf{J} \mathbf{v}\right|^2}{\mathbf{v}^H \mathbf{Q} \mathbf{v}}. \tag{8}$$

Lemma 1: The optimal solution of problem (8) is given by solving the equality $(\mathbf{I} - \mathbf{Q}^{-1}\mathbf{J})\mathbf{v} = \mathbf{0}$.

Proof: According to the positive definiteness of $\mathbf{Q}$, let $\mathbf{w} = \mathbf{Q}^{1/2}\mathbf{v}$ and $\mathbf{B} = \mathbf{Q}^{-1/2}\mathbf{J}\mathbf{Q}^{-1/2}$. Then the objective of (8) becomes $\frac{(\mathbf{w}^H \mathbf{B} \mathbf{w})^2}{\mathbf{w}^H \mathbf{w}}$. Observing that for the scalar $\mathbf{w}^H\mathbf{B}\mathbf{B}\mathbf{w} \in \mathbb{C}$, we have $(\mathbf{B}\mathbf{w}\mathbf{w}^H\mathbf{B})\mathbf{B}\mathbf{w} = (\mathbf{w}^H\mathbf{B}\mathbf{B}\mathbf{w})\mathbf{B}\mathbf{w}$, which implies that $\mathbf{B}\mathbf{w}$ is an eigenvector of the matrix $\mathbf{B}\mathbf{w}\mathbf{w}^H\mathbf{B}$. Since the matrix $\mathbf{B}\mathbf{w}\mathbf{w}^H\mathbf{B}$ is of rank one, it is obvious that $\frac{(\mathbf{w}^H\mathbf{B}\mathbf{w})^2}{\mathbf{w}^H\mathbf{w}} = \frac{\mathbf{w}^H(\mathbf{B}\mathbf{w}\mathbf{w}^H\mathbf{B})\mathbf{w}}{\mathbf{w}^H\mathbf{w}} \leq \lambda_{\max}(\mathbf{B}\mathbf{w}\mathbf{w}^H\mathbf{B})$, where $\lambda_{\max}$ is the maximum eigenvalue and the equality holds when $\mathbf{w} = \mathbf{B}\mathbf{w}$, i.e., $(\mathbf{I} - \mathbf{Q}^{-1}\mathbf{J})\mathbf{v} = \mathbf{0}$. The proof is complete. ∎

Once we obtain an optimal solution of (8), say $\mathbf{v}'$, from *Lemma 1*, the desired design of $\mathbf{v}$ with unit-magnitude elements for the IRSs can be subsequently achieved by using similar vector projection techniques as in [3]–[5]. As an alternative, we can directly extract the phase of $\mathbf{v}'$ to obtain $\mathbf{v}^* = \angle\mathbf{v}'$, which is computationally efficient and also gives close-to-optimal performance in most cases [5].

B. Ergodic Rate Analysis

Given the derived results in *Theorem 1*, we show that an insightful closed-form solution can be obtained for the special case with perfect CSI under uncorrelated Rician channels, which is summarized in the following Lemma.

Lemma 2: For an uncorrelated channel with $M = 1$ and perfect CSI at the transmitter, the ergodic achievable rate in (7) with the proposed statistical reflection design is given by

$$\bar{C} = \log_2\left(1 + \frac{P}{\sigma_w^2}(1 + \Upsilon_1)\right) \triangleq C_1, \tag{9}$$

when $\Upsilon_1 = L^2\left(\sum_{n=1}^{N} \sqrt{\frac{\alpha_n\beta_n K_{1n}K_{2,n}}{(K_{1,n}+1)(K_{2,n}+1)}}\right)^2 + L\sum_{n=1}^{N} \frac{\alpha_n\beta_n(K_{2,n}+K_{1,n}+1)}{(K_{1,n}+1)(K_{2,n}+1)}$.

Proof: See Appendix B. ∎

Remark 1: The result in (9) implies that the rate in (9) is solely determined by the large-scale fading coefficients and Rician factors. If the distances between the user and IRSs and between the BS and IRSs increase, equivalently with decreasing β_n, α_n, $K_{1,n}$, and $K_{2,n}$, the performance deteriorates. To shed light on the design of the distributed IRS system, we further consider the system performance under some special cases as follows.

Case 1 (Pure LoS Propagations): If both channels of BS-to-IRSs and IRSs-to-user are pure LoSs, i.e., $K_{1n} = \infty$ and $K_{2n} = \infty$, $\forall n = 1, \ldots, N$, the ergodic achievable rate in (9) reduces to

$$C_1^{\text{LoS}} = \log_2\left(1 + \frac{P}{\sigma_w^2}\left(1 + L^2\left(\sum_{n=1}^{N}\sqrt{\alpha_n\beta_n}\right)^2\right)\right). \tag{10}$$

The rate in (10) is proportional to L^2 as expected, but also depends on the large-scale fadings. When we set the normalized $\beta_n = \alpha_n = 1$, it gives $C_1^{\text{LoS}} = \log_2(1 + \frac{P}{\sigma_w^2}(1 + L^2N^2))$.

Case 2 (Pure Rayleigh Channels): If both channels of BS-to-IRSs and IRSs-to-user are Rayleigh distributed, i.e., $K_{1,n} = 0$ and $K_{2,n} = 0$, $\forall n = 1, \ldots, N$, in a rich-scattering scenario, the ergodic achievable rate reduces to

$$\begin{aligned} C_1^{\text{R}} &= \log_2\left(1 + \frac{P}{\sigma_w^2}\left(1 + L\sum_{n=1}^{N}\alpha_n\beta_n\right)\right) \\ &\leq \log_2\left(1 + \frac{P}{\sigma_w^2}(1 + LN)\right), \end{aligned} \tag{11}$$

where the inequality in (11) holds when we normalized $\alpha_n = \beta_n = 1$.

Remark 2: Comparing the above two cases, we observe that the achievable rate becomes proportional to L and N when both $\mathbf{H}$ and $\mathbf{g}$ are Rayleigh fading. When the LoS paths exist as in Case 1, the deployment of multiple IRSs improves the achievable rate significantly. Compared to a centralized deployment, distributed IRSs obviously increase the possibility of the presence of LoS channels.

Case 3 (Hybrid Propagation): For a general case, we define that the pure-LoS set $\mathcal{R}$. If $i \in \mathcal{R}$, we have BS-to-IRS j path and IRS j-to-user path are both LoS ($K_{1,j} = \infty$ and $K_{2,j} = \infty$, $j \in \mathcal{R}$), while the IRS in $\bar{\mathcal{R}} = \{1, \ldots, N\}\backslash\mathcal{R}$ only has one or zero LoS path ($K_{1,j} = \infty$ and $K_{2,j} = 0$ or $K_{1,j} = 0$ and $K_{2,j} = \infty$). Then, the ergodic achievable rate in (9) can be rewritten as

$$\begin{aligned} &C^{\text{Hybrid}} \\ &= \log_2\left(1 + \frac{P}{\sigma_w^2}\left(1 + L^2\left(\sum_{j\in\mathcal{M}}\sqrt{\alpha_j\beta_j}\right)^2 + L\sum_{n=1}^{N}\alpha_n\beta_n\right)\right) \\ &\leq \log_2\left(1 + \frac{P}{\sigma_w^2}(1 + L^2m^2 + LN)\right), \end{aligned} \tag{12}$$

where $m = |\mathcal{R}|$ is the cardinality of $\mathcal{R}$.

Remark 3: The result in (12) implies that the performance benefits brought by the distributed IRSs, rely on the presence of LoS paths. In practice, if only a subset of IRSs can be selected to serve a user, the IRSs that have clear LoS paths in the vicinity of the user should be selected to ensure better performance.

IV. Simulation Results

In this section, we provide numerical results to validate the theoretical derivations. We set $T = 10$, $\rho = 20$ dB, $\sigma_w^2 = 1$, $P = 20$ dB, $\beta_n = C_0(\frac{d_{1,n}}{D_0})^{-\alpha}$, and $\alpha_n = C_0(\frac{d_{2,n}}{D_0})^{-\alpha}$, where $C_0 = 10^{-3}$ is the path loss at the reference distance $D_0 = 1$ (m), $\alpha = 2.5$ is the pathloss exponent, $d_{1,n} \leq 10$ m and

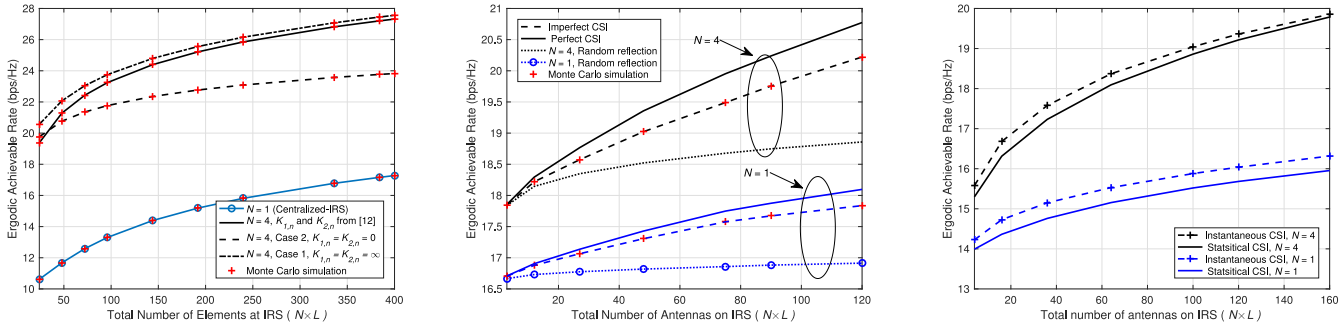

(a) (b) (c)

Fig. 1. (a) Perfect CSI with $M = 1$. (b) Different CSI setups with $M = 9$. (c) Perfect instantaneous CSI vs. statistival CSI.

$d_{2,n} \leq 20$ m are, respectively, the distance between the BS and IRS n, and the distance between the user and IRS n. The statistical correlation matrix is defined as in [1]. The Rician coefficents are set as $K_{1,n} = 10^{1.3-0.003d_{1,n}}$ and $K_{2,n} = 10^{1.3-0.003d_{2,n}}$ [9]. The IRSs are uniformly distributed in the cell coverage and simulation results are averaged with 1000 fading channel realizations to ensure fairness.

Fig. 1(a) cshows the ergodic achievable rate versus the total number of reflecting elements with perfect CSI. Solid lines correspond to analytical results under Rician fading channels while dotted markers correspond to Case 1 and Case 2. The system with 4 distributed IRSs, $N = 4$, outperforms the system with a centralized-IRS, i.e., $N = 1$, with the same total number of reflecting elements NL. As NL increases, the performance gap between the results in solid line and these in Case 1 diminishes, which agrees with the results in [4], where the gap is caused by the coefficients $\frac{K_{1n}K_{2,n}}{(K_{1,n}+1)(K_{2,n}+1)} < 1$ and $\frac{K_{1n}+K_{2,n}+1}{(K_{1,n}+1)(K_{2,n}+1)} < 1$ in (9) become less dominated. Besides, the gap between Case 1 and Case 2 enlarges since the SNR loss $N^2L^2\frac{P}{\sigma_w^2}$ in Case 2 is proportional to L^2, as predicted in *Remark 2* and *Remark 3*.

Fig. 1(b) shows the ergodic achievable rate versus the total number of reflecting elements. The analytical result in (7) tightly matches with the numerical results via Monte Carlo simulation. Besides, the considered distributed IRSs outperform the centralized-IRS. Compared with random reflection Φ_n, the results of our proposed reflection design are considerably higher due to the optimized phase shifts at IRSs. The approximation in our analysis is tight mainly because the dimensions of the matrices and vectors, i.e., $N \times L$, are very large, which satisfies the assumption of large antenna array for using the mathematical approximation.

For fair comparison, we compare the performance gains between instantaneous CSI and statistical CSI under the assumption of no channel estimation error for fairnes. With perfect instantaneous CSI, we exploit the solution in [12] to design the reflection vector in a SISO system. As shown in this new figure results, i.e., Fig. 1(c), we can find that the performance loss between the reflection design with instantaneous CSI and that with perfect statistical CSI are marginal.

V. Conclusion

We proposed a low-complexity reflection design for IRSs with statistical CSI. The derived ergodic achievable rate can accurately characterize the system performance of the distributed IRSs system, which outperforms the one with a centralized IRS with the same number of IRS elements.

Appendix A
Proof of Theorem 1

In order to facilitate the analysis, we apply the result in [9, Lemma 1] which proves that the approximation of $\mathbb{E}\{\log_2(1+\frac{X}{Y})\} \approx \log_2(1+\frac{\mathbb{E}\{X\}}{\mathbb{E}\{Y\}})$ is accurate enough for massive MIMO, e.g., with a large number of antennas NL and M. Hence, we can approximate the rate in (6) as

$$\bar{C} \approx \log_2\left(1 + P\frac{\mathbb{E}\{\|\hat{\mathbf{h}}_d^H + \mathbf{v}^H\hat{\mathbf{Z}}\|^2\}}{\sigma_w^2 + \frac{\mathbb{E}\{|(\mathbf{e}_d^H + \mathbf{v}^H\mathbf{E}_Z)(\hat{\mathbf{h}}_d + \hat{\mathbf{Z}}^H\mathbf{v})|^2\}}{\mathbb{E}\{\|\hat{\mathbf{h}}_d^H + \mathbf{v}^H\hat{\mathbf{Z}}\|^2\}}}\right). \quad (13)$$

To proceed, we first derive the numerator in (13) as

$$\begin{aligned}
&\mathbb{E}\{\|\hat{\mathbf{h}}_d^H + \mathbf{v}^H\hat{\mathbf{Z}}\|^2\} \\
&\overset{(a)}{=} \mathbb{E}\{\hat{\mathbf{h}}_d^H\hat{\mathbf{h}}_d\} + \mathbb{E}\{\mathbf{v}^H\hat{\mathbf{Z}}\hat{\mathbf{Z}}^H\mathbf{v}\} \\
&= \mathbb{E}\{\mathbf{h}_d^H\mathbf{h}_d\} + \mathbb{E}\{\mathbf{e}_d^H\mathbf{e}_d\} + \mathbf{v}^H\mathbb{E}\{\mathbf{E}_Z\mathbf{E}_Z{}^H\}\mathbf{v} + \mathbf{v}^H\mathbb{E}\{\mathbf{Z}\mathbf{Z}^H\}\mathbf{v} \\
&\overset{(b)}{=} M + M\xi + MNL\xi + \mathbf{v}^H\mathbb{E}\{\mathbf{Z}\mathbf{Z}^H\}\mathbf{v}, \quad (14)
\end{aligned}$$

where (a) exploits the independence between $\hat{\mathbf{h}}_d$ and $\hat{\mathbf{Z}}$ since $\mathbf{Z}$, $\mathbf{E}_Z$, $\mathbf{h}_d$, and $\mathbf{e}_d$ are independent, while (b) is due to $\mathbf{h}_d \sim \mathcal{CN}(\mathbf{0}, \mathbf{I}_M)$, $\mathbf{e}_d \sim \mathcal{CN}(\mathbf{0}, \xi\mathbf{I}_M)$, and $\mathbf{E}_Z \sim \mathcal{CN}(\mathbf{0}, \xi\mathbf{I}_{NL} \otimes \mathbf{I}_M)$ for large M, NL. Then, we evaluate $\mathbf{v}^H\mathbb{E}\{\mathbf{Z}\mathbf{Z}^H\}\mathbf{v}$ in (14) as follows

$$\begin{aligned}
&\mathbf{v}^H\mathbb{E}\{\mathbf{Z}\mathbf{Z}^H\}\mathbf{v} \\
&\overset{(a)}{=} \mathbf{v}^H(\bar{\mathbf{G}}\bar{\mathbf{H}}\bar{\mathbf{H}}^H\bar{\mathbf{G}}^H + \bar{\mathbf{G}}\mathbf{K}_1\mathbb{E}\{\widetilde{\mathbf{H}}\widetilde{\mathbf{H}}^H\}\mathbf{K}_1\bar{\mathbf{G}}^H \\
&\quad + \mathbf{K}_2\mathbb{E}\{\widetilde{\mathbf{G}}\bar{\mathbf{H}}\bar{\mathbf{H}}^H\widetilde{\mathbf{G}}^H\}\mathbf{K}_2 + \mathbf{K}_2\mathbb{E}\{\widetilde{\mathbf{G}}\mathbf{K}_1\widetilde{\mathbf{H}}\widetilde{\mathbf{H}}^H\mathbf{K}_1\widetilde{\mathbf{G}}^H\}\mathbf{K}_2)\mathbf{v} \\
&\overset{(b)}{=} \mathbf{v}^H(\bar{\mathbf{G}}\bar{\mathbf{H}}\bar{\mathbf{H}}^H\bar{\mathbf{G}}^H + M\bar{\mathbf{G}}\mathbf{K}_1\mathbf{R}\mathbf{K}_1\bar{\mathbf{G}}^H)\mathbf{v} \\
&\quad + \operatorname{tr}\{\mathbf{K}_2\bar{\mathbf{H}}\bar{\mathbf{H}}^H\mathbf{K}_2\} + M\operatorname{tr}\{\mathbf{K}_2\mathbf{K}_1\mathbf{R}\mathbf{K}_1\mathbf{K}_2\}, \quad (15)
\end{aligned}$$

where (a) exploits the independence between $\widetilde{\mathbf{G}}$ and $\widetilde{\mathbf{H}}$ and the fact that $\bar{\mathbf{G}}$ and $\bar{\mathbf{H}}$ are constants, and (b) follows by

$\widetilde{\mathbf{H}} \sim \mathcal{CN}(\mathbf{0}, \mathbf{R} \otimes \mathbf{I}_M)$ and the diagonality of $\widetilde{\mathbf{G}}$ whose entries are independent and identically distributed (i.i.d.) Gaussian distributed with zero mean and unit variance.

Substituting (15) into equation (14) yields

$$\begin{aligned}&\mathbb{E}\{\|\hat{\mathbf{h}}_d^H + \mathbf{v}^H\hat{\mathbf{Z}}\|^2\}\\&= (1+\xi)M + MNL\xi + \mathbf{v}^H(M\mathbf{K}_2\,\mathrm{tr}\{\mathbf{K}_1\mathbf{R}\mathbf{K}_1\}\mathbf{K}_2\\&\quad + M\bar{\mathbf{G}}\mathbf{K}_1\mathbf{R}\mathbf{K}_1\bar{\mathbf{G}}^H + \mathbf{K}_2\,\mathrm{tr}\{\bar{\mathbf{H}}\bar{\mathbf{H}}^H\}\mathbf{K}_2 + \bar{\mathbf{G}}\bar{\mathbf{H}}\bar{\mathbf{H}}^H\bar{\mathbf{G}}^H)\mathbf{v}.\end{aligned} \tag{16}$$

For the denominator in (13), we have

$$\begin{aligned}&\mathbb{E}\{|(\mathbf{e}_d^H + \mathbf{v}^H\mathbf{E}_{\mathrm{Z}})(\hat{\mathbf{h}}_d + \hat{\mathbf{Z}}^H\mathbf{v})|^2\}\\&= \mathbb{E}\{\mathbf{e}_d^H\hat{\mathbf{h}}_d\hat{\mathbf{h}}_d^H\mathbf{e}_d\} + \mathbb{E}\{\mathbf{v}^H\mathbf{E}_{\mathrm{Z}}\hat{\mathbf{h}}_d\hat{\mathbf{h}}_d^H\mathbf{E}_{\mathrm{Z}}{}^H\mathbf{v}\}\\&\quad + \mathbb{E}\{\mathbf{e}_d^H\hat{\mathbf{Z}}^H\mathbf{v}\mathbf{v}^H\hat{\mathbf{Z}}\mathbf{e}_d\} + \mathbb{E}\{\mathbf{v}^H\mathbf{E}_{\mathrm{Z}}\hat{\mathbf{Z}}^H\mathbf{v}\mathbf{v}^H\hat{\mathbf{Z}}\mathbf{E}_{\mathrm{Z}}{}^H\mathbf{v}\}.\end{aligned} \tag{17}$$

The four expectation terms in (17) can be, respectively, calculated as

$$\begin{aligned}&\mathbb{E}\{\mathbf{e}_d^H\hat{\mathbf{Z}}^H\mathbf{v}\mathbf{v}^H\hat{\mathbf{Z}}\mathbf{e}_d\} = \mathbf{v}^H\mathbb{E}\{\hat{\mathbf{Z}}\mathbf{e}_d\mathbf{e}_d^H\hat{\mathbf{Z}}^H\}\mathbf{v}\\&\quad = \xi\mathbf{v}^H\mathbb{E}\{\hat{\mathbf{Z}}\hat{\mathbf{Z}}^H\}\mathbf{v},\end{aligned} \tag{18}$$

$$\begin{aligned}&\mathbb{E}\{\mathbf{v}^H\mathbf{E}_Z\hat{\mathbf{Z}}^H\mathbf{v}\mathbf{v}^H\hat{\mathbf{Z}}\mathbf{E}_Z^H\mathbf{v}\}\\&\quad = \mathbf{v}^H\mathbb{E}\{\mathbf{Z}\mathbb{E}\{\mathbf{E}_{\mathrm{Z}}^H\mathbf{v}\mathbf{v}^H\mathbf{E}_{\mathrm{Z}}\mathbf{Z}^H\}\}\mathbf{v} + \mathbb{E}\{|\mathbf{v}^H\mathbf{E}_{\mathrm{Z}}\mathbf{E}_{\mathrm{Z}}^H\mathbf{v}|^2\}\\&\quad = \xi NL\mathbf{v}^H\mathbb{E}\{\mathbf{Z}\mathbf{Z}\}\mathbf{v} + \xi^2M(M+1)N^2L^2,\end{aligned} \tag{19}$$

$$\begin{aligned}&\mathbb{E}\{\mathbf{e}_d^H\hat{\mathbf{h}}_d\hat{\mathbf{h}}_d^H\mathbf{e}_d\} = \mathbb{E}\{\mathbf{e}_d^H\mathbf{h}_d\mathbf{h}_d^H\mathbf{e}_d\} + \mathbb{E}\{\mathbf{e}_d^H\mathbf{e}_d\mathbf{e}_d^H\mathbf{e}_d\}\\&\quad = \xi M + \xi^2M(M+1),\end{aligned} \tag{20}$$

and

$$\begin{aligned}&\mathbf{v}^H\mathbb{E}\{\mathbf{E}_{\mathrm{Z}}\hat{\mathbf{h}}_d\hat{\mathbf{h}}_d^H\mathbf{E}_{\mathrm{Z}}{}^H\}\mathbf{v}\\&\quad = \mathbf{v}^H\mathbb{E}\{\mathbf{E}_{\mathrm{Z}}\mathbf{h}_d\mathbf{h}_d^H\mathbf{E}_{\mathrm{Z}}{}^H\}\mathbf{v} + \mathbf{v}^H\mathbb{E}\{\mathbf{E}_{\mathrm{Z}}\mathbf{e}_d\mathbf{e}_d^H\mathbf{E}_{\mathrm{Z}}{}^H\}\mathbf{v}\\&\quad = MNL\xi + MNL\xi^2 = (1+\xi)\xi MNL,\end{aligned} \tag{21}$$

where the last equality in (19) holds because $\mathbf{v}^H\mathbf{Z} \sim \mathcal{CN}(\mathbf{0}, \xi NL\mathbf{I}_M)$ and we obtain $\mathbb{E}\{w(\xi NL)^{-1}w\} = M(M+1)NL\xi$, i.e., $\mathbb{E}\{|\mathbf{v}^H\mathbf{E}_{\mathrm{Z}}\mathbf{E}_{\mathrm{Z}}^H\mathbf{v}|^2\} = \xi^2M(M+1)N^2L^2$ as $w \triangleq \mathbf{v}^H\mathbf{E}_{\mathrm{Z}}\mathbf{E}_{\mathrm{Z}}^H\mathbf{v}$ is an uncorrelated central Wishart random variable, commonly denoted as $w \sim \mathcal{CW}_1(M, NL\xi)$ [13].

Substituting (20) and (19) into (15) and using (14), we have

$$\begin{aligned}&\mathbb{E}\{|(\mathbf{e}_d^H + \mathbf{v}^H\mathbf{E}_{\mathrm{Z}})(\hat{\mathbf{h}}_d + \hat{\mathbf{Z}}^H\mathbf{v})|^2\}\\&\quad = \xi M + \xi^2M(M+1) + (1+\xi)MNL\xi + \xi^2MNL\\&\quad\quad + (\xi + NL\xi)\mathbf{v}^H\mathbf{C}\mathbf{v} + M(M+1)N^2L^2\xi^2,\end{aligned} \tag{22}$$

where $\mathbf{C} = \bar{\mathbf{G}}\bar{\mathbf{H}}\bar{\mathbf{H}}^H\bar{\mathbf{G}}^H + M\bar{\mathbf{G}}\mathbf{K}_1\mathbf{R}\mathbf{K}_1\bar{\mathbf{G}}^H + \frac{1}{NL}\,\mathrm{tr}\{\mathbf{K}_2\bar{\mathbf{H}}\bar{\mathbf{H}}^H\mathbf{K}_2\} + \frac{M}{NL}\,\mathrm{tr}\{\mathbf{K}_2\mathbf{K}_1\mathbf{R}\mathbf{K}_1\mathbf{K}_2\}$. Now by substituting (16) and (22) into (13), we complete the proof.

APPENDIX B
PROOF OF LEMMA 2

The ergodic rate in (7) with perfect CSI for beamforming design, i.e., $\xi = 0$, can be rewritten as $\bar{C} = \log_2(1 + \frac{P}{\sigma_w^2}(M + \mathbf{v}^H\mathbf{C}\mathbf{v}))$.

Considering the term $s \triangleq \mathbf{v}^H\mathbf{C}\mathbf{v}$, we have

$$\begin{aligned}s &= \left\|\mathbf{v}^H\bar{\mathbf{G}}\bar{\mathbf{H}}\right\|^2 + \mathrm{tr}\{\bar{\mathbf{G}}\mathbf{K}_1\mathbf{K}_1\bar{\mathbf{G}}^H\}\\&\quad + \mathrm{tr}\{\bar{\mathbf{H}}\bar{\mathbf{H}}^H\mathbf{K}_2\mathbf{K}_2\} + \mathrm{tr}\{\mathbf{K}_2\mathbf{K}_1\mathbf{K}_1\mathbf{K}_2\}\\&= \left(\sum_{n=1}^{N}\left(\sqrt{\frac{\alpha_n\beta_nK_{1,n}K_{2,n}}{(K_{1,n}+1)(K_{2,n}+1)}}\sum_{i=1}^{L}e^{j\phi_{ni}+j\theta_{ni}^g+j\theta_{ni}^H}\right)\right)^2\\&\quad + \sum_{n=1}^{N}\left(\frac{L\alpha_n\beta_nK_{2,n}}{(K_{1,n}+1)(K_{2,n}+1)} + \frac{L\alpha_n\beta_nK_{1,n}}{(K_{1,n}+1)(K_{2,n}+1)}\right)\\&\quad + \sum_{n=1}^{N}\left(\frac{L\alpha_n\beta_n}{(K_{1,n}+1)(K_{2,n}+1)}\right)\\&\le L^2\left(\sum_{n=1}^{N}\sqrt{\frac{\alpha_n\beta_nK_{1,n}K_{2,n}}{(K_{1,n}+1)(K_{2,n}+1)}}\right)^2\\&\quad + L\sum_{n=1}^{N}\frac{\alpha_n\beta_n(K_{1,n}+K_{2,n}+1)}{(K_{1,n}+1)(K_{2,n}+1)},\end{aligned} \tag{23}$$

where $\theta_{ni}^H = \angle\bar{\mathbf{H}}_{ni}$ and $\theta_{ni}^g = \angle\bar{\mathbf{g}}_{ni}$ are the angles of the small-scale fading coefficients of $\bar{\mathbf{H}}$ and $\bar{\mathbf{g}}$, respectively. The inequality in (23) holds with equality if and only if $\mathbf{v}$ is designed by: $\phi_{ni} = -(\theta_{ni}^g + \theta_{ni}^H)$, $n = \{1, \ldots, N\}$, and $i = \{1, \ldots, L\}$. This completes the proof.

REFERENCES

[1] D. W. K. Ng, E. S. Lo, and R. Schober, "Energy-efficient resource allocation in OFDMA systems with large numbers of base station antennas," *IEEE Trans. Wireless Commun.*, vol. 11, no. 9, pp. 3292–3304, Sep. 2012.

[2] S. Zhou, W. Xu, K. Wang, M. Di Renzo, and M.-S. Alouini, "Spectral and energy efficiency of IRS-assisted MISO communication with hardware impairments," *IEEE Wireless Commun. Lett.*, vol. 9, no. 9, pp. 1366–1369, Sep. 2020.

[3] Q. Wu and R. Zhang, "Intelligent reflecting surface enhanced wireless network: Joint active and passive beamforming design," in *Proc. IEEE GLOBECOM*, Abu Dhabi, UAE, Oct. 2018, pp. 1–6.

[4] Y. Han, W. Tang, S. Jin, C. Wen, and X. Ma, "Large intelligent surface-assisted wireless communication exploiting statistical CSI," *IEEE Trans. Veh. Technol.*, vol. 68, no. 8, pp. 8238–8242, Aug. 2019.

[5] D. Mishra and H. Johansson, "Channel estimation and low-complexity beamforming design for passive intelligent surface-assisted MISO wireless energy transfer," in *Proc. IEEE ICASSP*, May 2019, pp. 4659–4663.

[6] S. Zhou, W. Xu, K. Wang, C. Pan, M.-S. Alouini, and A. Nallanathan, "Ergodic rate analysis of cooperative ambient backscatter communication," *IEEE Wireless Commun. Lett.*, vol. 8, no. 6, pp. 1679–1682, Dec. 2019.

[7] J. Lyu and R. Zhang, "Hybrid active/passive wireless network aided by intelligent reflecting surface: System modeling and performance analysis," 2020. [Online]. Available: https://arxiv.org/abs/2004.13318.

[8] J. Lyu and R. Zhang, "Spatial throughput characterization for intelligent reflecting surface aided multiuser system," *IEEE Wireless Commun. Lett.*, vol. 9, no. 6, pp. 834–838, Jun. 2020.

[9] Q. Zhang, S. Jin, and K.-K. Wong, "Power scaling of uplink massive MIMO systems with arbitrary-rank channel means," *IEEE J. Sel. Topics Signal Process.*, vol. 8, no. 5, pp. 966–981, Oct. 2014.

[10] T. C. Mai, H. Q. Ngo, and T. Q. Duong, "Downlink spectral efficiency of cell-free massive MIMO systems with multi-antenna users," in *Proc. IEEE GlobalSIP*, 2018, pp. 828–832.

[11] O. Raeesi and A. Gokceoglu, "Performance analysis of multi-user massive MIMO downlink under channel non-reciprocity and imperfect CSI," *IEEE Trans. Commun.*, vol. 66, no. 6, pp. 2456–2471, Jun. 2018.

[12] E. Björnson, Ö. Özdogan, and E. G. Larsson, "Intelligent reflecting surface versus decode-and-forward: How large surfaces are needed to beat relaying?" *IEEE Wireless Commun. Lett.*, vol. 9, no. 2, pp. 244–248, Feb. 2020.

[13] D. K. Nagar and A. K. Gupta, "Expectations of functions of complex wishart matrix," *Acta Applicandae Mathematicae*, vol. 113, pp. 265–288, Mar. 2011.